Applied Mathematics, Modeling and Computer Simulation
C.-H. Chen et al. (Eds.)

doi:10.3233/ATDE221116

Numerical Study of the Propagating Properties of a Laser-Generated Surface Acoustic Wave Interacting with a Bracket Structure

Ziming LI[1]
Faculty of Materials and Manufacturing, Beijing University of Technology, Beijing, China

Abstract. Shield tunneling machines are widely used around the world for construction in tunnels, railways, and subways. The bracket of a shield tunneling machine, which is welded to the cutterhead, is prone to suffer maximum stress due to its bad operating environment. This paper introduces a laser-generated surface acoustic wave for non-destructive detection. A numerical model is constructed to analyze the interaction between a laser-generated surface acoustic wave and a bracket structure. The results show that the laser-generated acoustic wave with a longitudinal wave, a shear wave, and a Rayleigh wave can propagate along the surface of the bracket structure. When the wave encounters the junction of the welding and the horizontal surface, it generates a reflected wave, a transmitted wave, and a mode converted wave. This propagating phenomenon can be used for the defect detection of a bracket in the future.

Keywords. Bracket, cutterhead, laser-generated surface wave, finite element method, interaction

1. Introduction

The shield tunneling method has been widely used for construction in tunnels, railways, and subways due to its high efficiency, full automation, minimum effects on ground structures [1]. As the core component, the cutterhead is very important. During engineering projects, the cutterhead breaks and cuts the soil with the comprehensive action of thrust and torque using the cutters. Due to the complex geological surrounding conditions, the long running time makes it easy for fatigue operations to occur [2]. Fatigue cracks or other types of defects will be generated, subsequently leading to potential risks. If these defects are not detected on time, huge catastrophic consequences will occur. It is thus necessary to detect the defects in the cutterhead components of shield tunneling machines.

The laser-generated surface acoustic wave detection method is a method with growing popularity that has made a breakthrough in the detection of the surface and subsurface defects of a structure, and this method has attracted wide attention. It is

[1] Corresponding Author, Ziming LI, Faculty of Materials and Manufacturing, Beijing University of Technology, Beijing, China; E-mail: liziming@bjut.edu.cn.

especially suitable for the detection of the surface cracks of a large structure. It has the advantages of combining laser and ultrasonic detection technology benefits such as being non-contact and having flexible excitation and detection, a wide detection signal band, and high spatial and temporal resolution [3]. The interaction of the laser beam and the material generates the surface acoustic wave. According to the incident laser power density and solid surface conditions, the excitation mechanisms in metal materials are generally divided into the thermoelastic mechanism and the ablation mechanism [4]. For the thermal mechanism, the laser beam has exposure to the surface of the structure, and the laser power density is lower than the material surface damage threshold. The surface of the material is nondestructive; so, it is more suitable for the nondestructive detection of a structure.

Li et al. [5] conducted a numerical static analysis of a cutterhead. It could be seen from the analysis that the local maximum stress was located on the inner side of the cutterhead beam support plate; this could suggest the dangerous position where the cutterhead was prone to crack. Li et al. [6] presented a finite element analysis for the maximum thrust condition. The flange of the cutterhead was fixed, the three loads of the cutters were loaded on the seat, and the maximum stress position of the front panel of the cutterhead appeared on the edge of the cutter seat. In summary, all the key parts that were prone to breakage had one thing in common; they all tended to be located in the welding parts.

This paper takes a bracket component as a typical part that is easier to generate cracks for. A numerical study is presented in the following sections. The propagating properties of a laser-generated surface acoustic wave traveling in a bracket are discussed.

2. Theory and Numerical Model

2.1. Thermal Conduction Theory

The principle of the thermoelastic mechanism is that a single laser pulse illuminates the structure with a power density less than the melting threshold of the material. Parts of the energy are reflected, and others penetrate the structure, generating a non-uniform temperature field and then resulting in a stress field with ultrasonic waves propagating in the structure.

The thermal conductivity equation can be used to calculate the generated temperature field accurately. In a cylindrical coordinate system, this equation can be expressed as follows:

$$\rho c \frac{\partial T(r,z,t)}{\partial t} = \frac{1}{r}\frac{\partial}{\partial r}\left(rk \frac{\partial T(r,z,t)}{\partial r} \right) + \frac{\partial}{\partial z}\left(k \frac{\partial T(r,z,t)}{\partial z} \right) \tag{1}$$

where $T(r,z,t)$ is the temperature distribution at moment t, ρ is the density, c is the specific heat, and k is the thermal conductivity.

The boundary and initial temperature conditions are expressed as follows:

$$-k \frac{\partial T(r,z,t)}{\partial z}\Big|_{z=0} = I_0(1-R) f(r) g(t) \tag{2}$$

$$\partial T(r,z,t)/\partial z \big|_{z=h} = 0 \tag{3}$$

$$T(r,z,0)=300\ \mathrm{K} \tag{4}$$

where I_0 is the energy flow of the laser that is loaded on the surface of the structure, R is the reflection coefficient of the material, h is the thickness of the structure, $f(r)$ is the spatial distribution of the laser pulse, and $g(t)$ is the time distribution of the laser pulses.

Once the temperature field is calculated, the stress field can be obtained by taking the generated temperature field as the load. This can be expressed by the Navier-Stokes equation in a thermoelastic body, as follows:

$$\begin{aligned}(\lambda+2\mu)\nabla(\nabla\cdot U(r,z,t))-\mu\nabla\times\nabla\times U(r,z,t)\\ -\alpha(3\lambda+2\mu)\nabla T(r,z,t)=\rho\frac{\partial^2 U(r,z,t)}{\partial^2 t}\end{aligned} \tag{5}$$

where λ and μ are the Lame constants, and α is the thermal expansion.

In addition, the top and bottom surfaces should satisfy the following boundary displacement conditions:

$$\vec{n}\cdot\left[\sigma-(3\lambda+2\mu)\alpha T(r,z,t)I\right]=0 \tag{6}$$

where $\boldsymbol{n}$ is the unit vector normal to the surface, $\boldsymbol{I}$ is the unit tensor, and σ is the stress tensor.

The initial condition for the displacement field is given by

$$U(r,z,t)\big|_{t=0}=\frac{\partial U(r,z,t)}{\partial t}\Big|_{t=0}=0 \tag{7}$$

2.2. Numerical Model

According to the thermal conduction theory described above, the thermal conduction equation and the control equation can be transformed as follows:

$$[C]\{T\}+[K_T]\{\dot{T}\}=\{p_1\}+\{p_2\} \tag{8}$$

$$[K]\{\vec{U}\}+[M]\{\ddot{\vec{U}}\}=\{F_{\mathrm{ext}}\} \tag{9}$$

where $[C]$ is the specific heat matrix, $[K_T]$ is the thermal conductivity matrix, $[K]$ is the stiffness matrix, $[M]$ is the mass matrix, $\{T\}$ is the temperature vector, $\{\dot{T}\}$ is the change rate vector with temperature, $\{p_1\}$, $\{p_1\}$ are the heat source vectors, $\{\vec{U}\}$ is the displacement vector, $\{\ddot{\vec{U}}\}$ is the acceleration vector, and $\{F_{\mathrm{ext}}\}$ is the external force vector. For thermoelasticity, the external force vector is expressed as follows:

$$\int_V [B]^{tr}[D]\{\varepsilon_0\}dV \tag{10}$$

where $[B]^{\mathrm{tr}}$ is the transpose of the shape functions, $[D]$ is the material matrix, and $\{\varepsilon_0\}$ is the thermal strain vector.

3. Parameters of Laser and Material

Based on the thermoelastic theories and models described above, the 2D finite element model of a bracket component in a cutterhead is constructed. The simplified schematic diagram of the bracket structure is shown in figure 1. The sizes of the structure refer to

Zhang et al. [7]. The structure is made of Q345 steel. The material parameters used in the finite element model are set as shown in table 1.

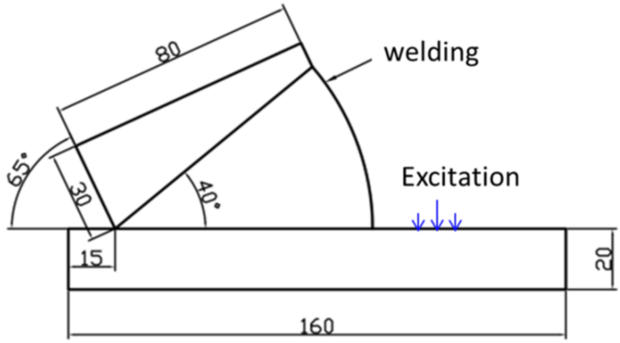

Figure 1. Simplified schematic diagram of the bracket structure

Table 1. Material parameters used in the finite element model

Density (kg/m^3)	Thermal expansion (1/K)	Specific heat (J/(kg•K))	Thermal conductivity (W/(m•K))	Young's modulus (Pa)	Poisson's ratio	Reflective coefficient
7850	1.4e-5	451	45.7	210e9	0.3	0.8

The excitation is located on the horizontal steel plate, and the horizontal distance from the exciting position to the welding is 25 mm. The pulsed laser is loaded on the excitation with the energy flow. The spatial distribution and the time distribution of the pulsed laser are assumed to have a Gaussian distribution, and their expressions are as follows:

$$\mathrm{f}(r) = \frac{2}{a_0\sqrt{2\pi}}\exp\left(-\frac{2r^2}{a_0{}^2}\right) \tag{11}$$

$$g(t) = \frac{8t^3}{t_0^4}\exp\left(-\frac{2t^2}{t_0^2}\right) \tag{12}$$

where a_0 is the radius of the laser pulse and is set to 500 μm, and t_0 is the rise time of the laser pulse and is set to 10 ns. The energy of the laser pulse is 50 mJ.

The receiving points are distributed on the horizontal steel plate with a step length of 1 mm and on the surface of the welding with a step length of 1°.

The mesh size and the time step in this numerical model should satisfy the criterion [8]. To ensure both the calculation time and the validity of the solution, a variable mesh size is adopted. First, the grid is meshed from dense to sparse from the surface to the bottom boundary. Then, the surface part meshes into dense and sparse grids according to whether the grid is located in the laser radiation region. Finally, a grid transition region with a free triangle element type is assigned between these dense and sparse regions. In this model, the mesh size of the ultrasonic propagation region on the surface layer was set to 50 μm and gradually transitioned to the bottom layer, which is 100 μm. The mesh size of the laser exciting area is set as 1 μm to ensure the accuracy of the calculation.

For the selection of the time step, it should be small enough to have a transient response to the temperature field generated by the heat source and to maintain high computational efficiency. Thus, a variable time step is used in this model, and its variation range is 0.1–10 ns.

4. Results and Discussions

4.1. Analysis of Temperature Field

Figure 2 shows the non-uniform transient temperature field distribution generated by a pulsed laser at 7 μs in the bracket component. This is the main reason for generating thermal stress. As shown in the figure, it can be seen that the maximum temperature is distributed on the surface of the structure. It is obvious that the diffusion length of the temperature in the horizontal direction is greater than that in the depth direction.

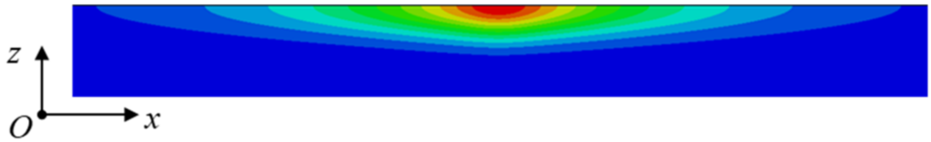

Figure 2. Temperature field distributions in the bracket component at 7 μs

4.2. Analysis of Displacement Field

The displacement fields at different times in the bracket of the cutterhead are obtained by providing the nodal thermal loads with an initial thermal analysis, as shown in figure 3.

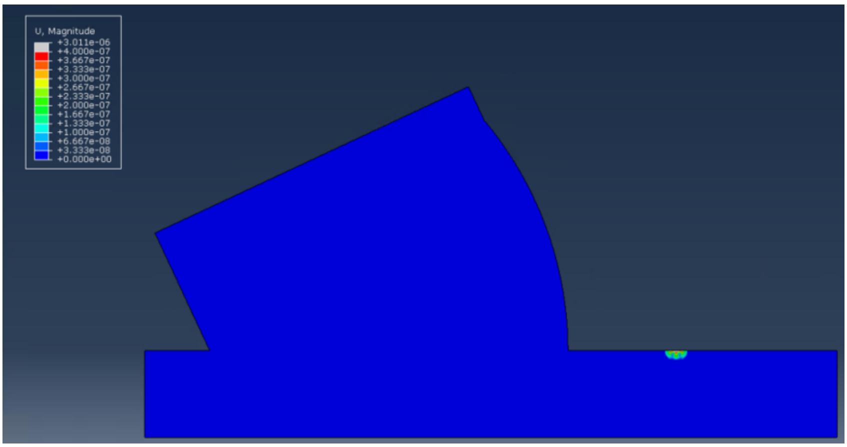

(a)-0.5 μs

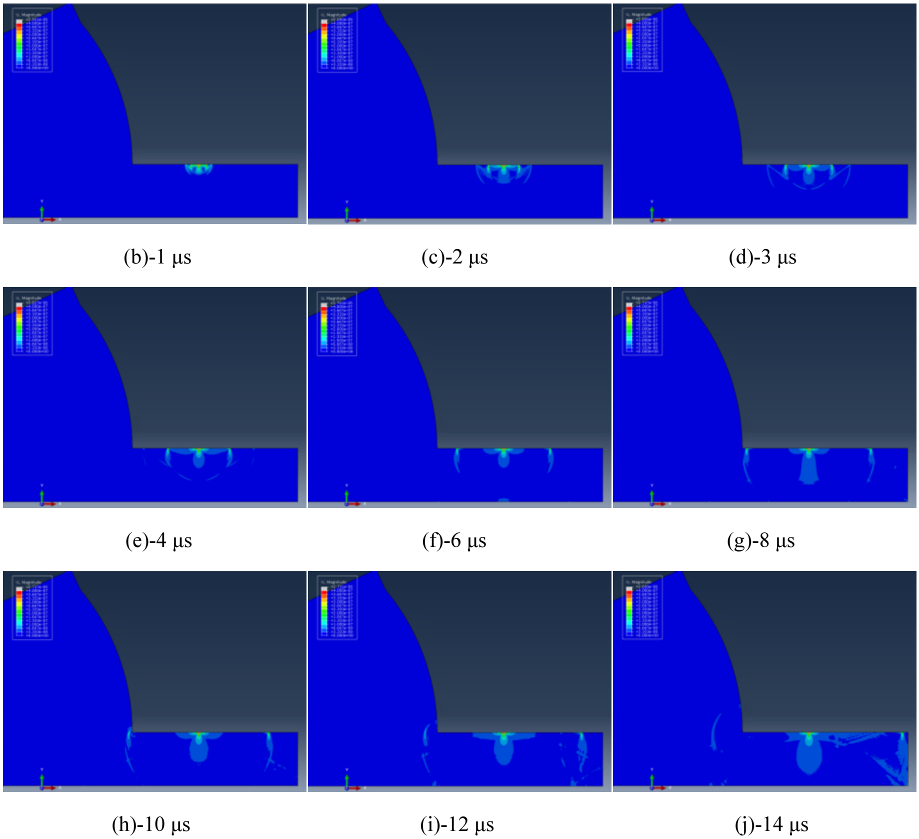

Figure 3. Displacement field in the bracket of cutterhead at different times

Figure 3(a) shows the whole bracket structure part, and (b)–(j) show the zoomed-in area to make it clearer for observation of the displacement field. It can be seen that the laser-generated acoustic wave propagates along the horizontal surface. The propagation wave later encounters the welding joint and then travels along the welding arc.

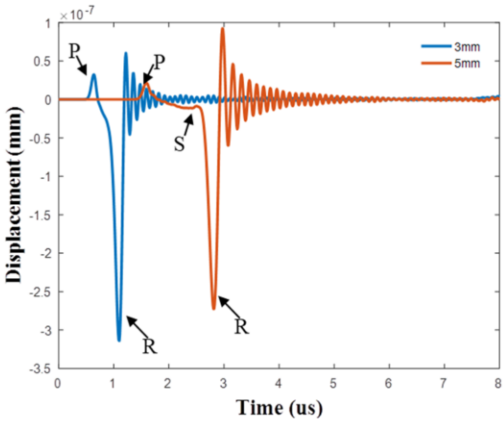

Figure 4. Out-of-plane displacements at the distances of 3 mm and 8 mm between the excitation and the receiver

To explore the detailed wave modes between the generated acoustic wave and the bracket structure, the out-of-plane displacements at the distances of 3 mm and 8 mm between the excitation and receiver on the horizontal surface are shown in figure 4. The laser-generated acoustic wave mainly contains three wave modes: longitudinal wave (P), shear wave (S), and Rayleigh wave (R). According to the arrival time in each waveform, the wave modes are labeled as shown in figure 4. The calculated velocities of P, S, and R in steel are 5262.6 m/s, 3200 m/s, and 2923.98 m/s, respectively.

Figure 5 shows the waterfall plot of the receiving point on the horizontal surface and the welding surface. As shown in the figure, the laser-generated surface acoustic wave propagates to the junction of the welding arc surface and the horizontal surface along with a longitudinal wave and a tiny shear wave. When it encounters the junction, the acoustic wave interacts with the welding and undergoes mode conversion. The out-of-plane displacements at positions 5° and 10° on the arc surface are taken as examples. The arrival times of these wave packets at position 5° are 7.13 μs, 10.02 μs, and 11.04 μs, respectively, and the arrival times of these wave packets at position 10° are 9.54 μs, 11.38 μs, and 13.46 μs, respectively. According to the calculation, the velocity of the first wave packet is 2997.93 m/s. This is the Rayleigh wave named RP, which is mode converted from the longitudinal wave. The velocity of the second wave packet is 5312.5 m/s. This is the longitudinal wave named PR, which is mode converted from the Rayleigh wave. The velocity of the third wave packet is 2985.54 m/s. This is the Rayleigh wave named RR, which is the transmitted wave from the Rayleigh wave. Similarly, it can be determined that part of the reflected wave is propagated back along the horizontal surface, which is named rR.

As described above, figure 6 depicts the detailed propagating properties of the laser-generated surface acoustic wave interacting with the bracket structure.

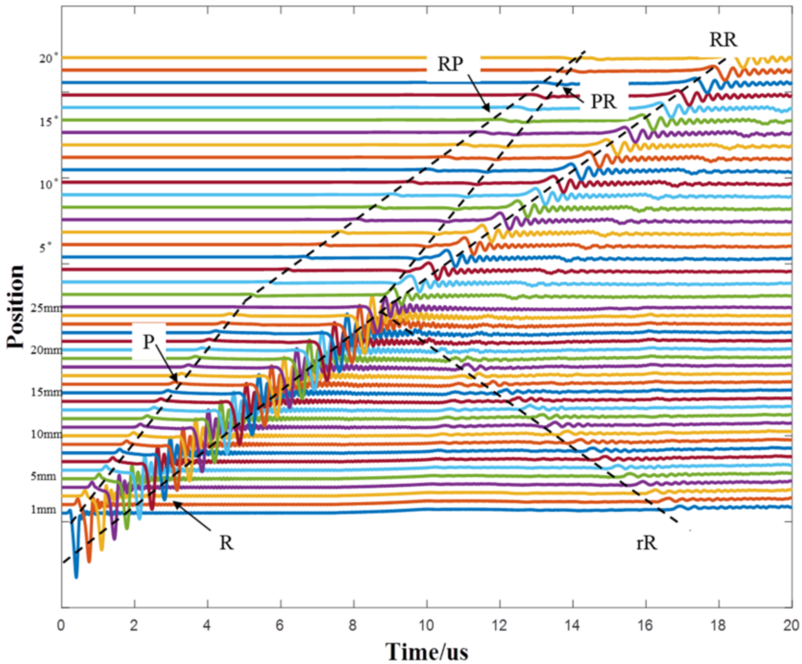

Figure 5. Waterfall plot of the receiving point on the horizontal surface and the welding surface

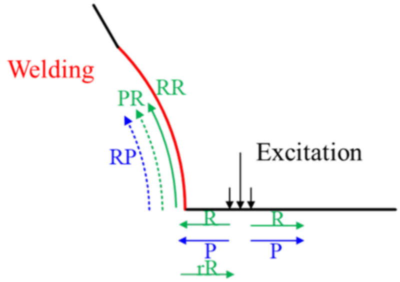

Figure 6. Detailed propagating properties of laser-generated surface acoustic wave interacting with the bracket structure

5. Conclusion

This paper presents a numerical study of the interaction between a laser-generated surface acoustic wave and the bracket component in a cutterhead. The basic thermoelastic theory and the finite element model are described. The results show that the displacement field is induced by the laser energy. A laser-generated acoustic wave with a longitudinal wave, a shear wave, and a Rayleigh wave propagates along the surface of the bracket structure. When the acoustic wave encounters the junction of the welding and the horizontal surface, it generates a reflected wave, a transmitted wave, and a mode converted wave. This propagating phenomenon can be used in the defect detection of a bracket.

Acknowledgments

This paper was supported by the National Natural Science Foundation of China (Grant No. 51905013).

References

[1] Zhou C, Kong T, Zhou Y, et al. Unsupervised spectral clustering for shield tunneling machine monitoring data with complex network theory[J]. Automation in construction, 2019, 11(107): 102924

[2] Shi H, Yang H, Gong G, et al. Determination of the cutterhead torque for EPB shield tunneling machine[J]. Automation in Construction, 2011, 20(8): 1087-1095

[3] Chen K, Fu X, Dorantes-Gonzalez D J, et al. Laser-generated surface acoustic wave technique for crack monitoring-A review[J]. International Journal of Automation Technology, 2013, 7(2):211-220

[4] Castellini P, Revel G M, Scalise L, et al. Experimental and numerical investigation on structural effects of laser pulses for modal parameter measurement[J]. Optics and Lasers in Engineering, 2000, 32(6): 565-581

[5] Li J, Zhang Z, Liu C, et al. Numerical failure analysis and fatigue life prediction of shield machine cutterhead[J]. Materials, 2021, 14(17): 4822

[6] Li J B, Zhang Z, Meng Z, et al. Tunnel boring machine cutterhead crack propagation life prediction with time integration method[J]. Advances in Mechanical Engineering, 2019, 11(6): 1-14

[7] Zhang Y X, Gao W, Wang D, et al. Three-Dimensional Simulation on the Welding Process of the Cutter-Head's Typical Position[J]. Machinery Design & Manufacture, 2015(5): 239-241

[8] Liu P, Wahab Nazirah A, Sohn Hoon. Numerical simulation of damage detection using laser-generated ultrasound[J]. Ultrasonics, 2016, 69: 248-258